Elastic Interaction between a Mesoscale Eddy-Pair and a Cyclonic Eddy

Zoeller Victoria Christine[1] and Viudez Alvaro[2]

[1]Institute of Marine Sciences
[2]Institute of Marine Sciences, Spain

November 16, 2022

Abstract

We investigate numerically the elastic interaction between an eddy-pair and an axisymmetrical cyclonic eddy in inviscid isochoric two-dimensional (2D), as well as in three-dimensional (3D) flows under the quasi-geostrophic (QG) approximation. The eddy-pair is a straight moving Lamb-Chaplygin dipole where the absolute value of either its positive or negative amount of vorticity equals the vorticity of the axisymmetrical eddy. The results for the 2D and 3D cases show that interactions with almost no vorticity exchange or vorticity loss to the background field between ocean eddies, but changing their displacement velocity, are possible. When the eddy-pair approaches the axisymmetrical eddy, their respective potential flows interact, the eddy-pair's trajectory acquires curvature and their vorticity poles separate. In the QG dynamics, the eddies suffer little vertical deformation, being the barotropic effects dominant. At the moment of highest interaction, the anticyclonic eddy of the pair elongates, simultaneously, the cyclonic eddy of the pair evolves towards spherical geometry, and the axisymmetrical eddy acquires prolate ellipsoidal geometry in the vertically stretched QG space. Once the eddy-pair moves away from the axisymmetrical eddy, its poles close, returning to their original geometry, and the anticyclonic and cyclonic eddy continue as an eddy-pair with a straight trajectory but along a new direction. The interaction is sensitive to the initial conditions and, depending on the initial position of the eddy-pair, as well as on small changes in the vorticity distribution of the axisymmetrical eddy, inelastic interactions may instead occur.

Elastic Interaction between a Mesoscale Eddy-Pair and a Cyclonic Eddy

V. Zoeller[1], A. Viúdez[1]

[1]Department of Physical Oceanography and Technology, Institute of Marine Sciences, CSIC, Barcelona 08003, Spain

Key Points:

- Numerical description of an elastic interaction between an eddy-pair and an axisymmetrical eddy in rotating quasi-geostrophic dynamics
- Numerical description of an elastic interaction between an eddy-pair and an axisymmetrical cyclonic eddy in two-dimensions
- Numerical simulations of inelastic interactions with vortex partner exchange, merging and straining out processes in two-dimensional flows

Corresponding author: Victoria Zoeller, `zoeller@icm.csic.es`

Abstract

We investigate numerically the elastic interaction between an eddy-pair and an axisymmetrical cyclonic eddy in inviscid isochoric two-dimensional (2D), as well as in three-dimensional (3D) flows under the quasi-geostrophic (QG) approximation. The eddy-pair is a straight moving Lamb-Chaplygin dipole where the absolute value of either its positive or negative amount of vorticity equals the vorticity of the axisymmetrical eddy. The results for the 2D and 3D cases show that interactions with almost no vorticity exchange or vorticity loss to the background field between ocean eddies, but changing their displacement velocity, are possible. When the eddy-pair approaches the axisymmetrical eddy, their respective potential flows interact, the eddy-pair's trajectory acquires curvature and their vorticity poles separate. In the QG dynamics, the eddies suffer little vertical deformation, being the barotropic effects dominant. At the moment of highest interaction, the anticyclonic eddy of the pair elongates, simultaneously, the cyclonic eddy of the pair evolves towards spherical geometry, and the axisymmetrical eddy acquires prolate ellipsoidal geometry in the vertically stretched QG space. Once the eddy-pair moves away from the axisymmetrical eddy, its poles close, returning to their original geometry, and the anticyclonic and cyclonic eddy continue as an eddy-pair with a straight trajectory but along a new direction. The interaction is sensitive to the initial conditions and, depending on the initial position of the eddy-pair, as well as on small changes in the vorticity distribution of the axisymmetrical eddy, inelastic interactions may instead occur.

Plain Language Summary

Ocean swirls, also known as eddies or vortices are ubiquitous in all oceans. Often they drift as two vortices together, rotating in opposite directions, known as eddy-pairs. The eddy-pair can interact with different vortical structures. Here we prove that elastic interactions between two vortices are possible, meaning that the interaction does not change the vorticity properties of the vortices. In particular, the interaction is between an eddy-pair and an axisymmetrical cyclonic eddy. We use the quasi-geostrophic three-dimensional dynamics as well as a two-dimensional model. We also describe numerically, in two-dimensions, inelastic interactions, where the eddy-pair separates or loses part of its vorticity.

1 Introduction

Mesoscale and submesoscale vortical structures are ubiquitous in the oceans and atmosphere. In particular, cyclonic and anticylonic vortices are found in different configurations, including monopoles, dipoles, and tripoles. For example, a dipole is made up of an anticyclone and a cyclone, drifting together as one vortex structure. They are also known as eddy-pairs, vortex pairs or couples, double vortices, modons, or mushroom-like vortices and have been observed all over the oceans. Some examples include eddy-pairs of the southern coast of Madagascar (de Ruijter et al., 2004; Ridderinkhof et al., 2013), eastern of Australia (Li et al., 2020), the Norwegian coast (Johannessen et al., 1989), the Mexican coast (Santiago-García et al., 2019), California coast (Sheres & Kenyon, 1989), in the Alaska current (Ahlnäs et al., 1987), in the South China Sea (Huang et al., 2017) and along the Canary Islands (Barton et al., 2004). These eddy-pairs are generated by different causes, including the instability of baroclinic currents (Carton, 2001), localized forcing in a viscous stratified fluid (Voropayev & Afanasyev, 1994), or coastal interaction (de Ruijter et al., 2004).

The dipole structure and its stability has been subject of many experimental, laboratory, and numerical studies (Couder & Basdevant, 1986; Flór & Van Heijst, 1994; Rasmussen et al., 1996; Voropayev & Afanasyev, 1994). The eddy-pair or dipole possesses a propagation speed, and may be considered as the simplest self-induced trans-

lating vortex structure (Afanasyev, 2003; Carton, 2001). For this reason it can interact with, for example, a sloping boundary (Kloosterziel et al., 1993), a submarine mountain (Zavala Sansón & Gonzalez, 2021), a coastline (de Ruijter et al., 2004), inertia–gravity waves (Claret & Viúdez, 2010; Huang et al., 2017), other dipoles (Afanasyev, 2003; Dubosq & Viúdez, 2007; McWilliams & Zabusky, 1982; Velasco Fuentes & Heijst, van, 1995; Voropayev & Afanasyev, 1992) or other multipolar vortices (Besse et al., 2014; Viúdez, 2021; Voropayev & Afanasyev, 1992). Most of these interactions seem to be inelastic, in the sense that the vorticity of the eddy-pair suffers irreversible changes during the interaction, for example during vortex merging or partial or complete straining out processes (Dritschel, 1995; Dritschel & Waugh, 1992; Dubosq & Viúdez, 2007; McWilliams & Zabusky, 1982; Voropayev & Afanasyev, 1992). However, in many instances ocean vortices do not interact strongly with one another for long time periods (Carton, 2001). Consequently, elastic interactions, where vorticity exchange does not occur, are also possible between ocean vortices. The works mentioned before describe in detail inelastic interactions lacking the description of elastic interactions. In this study we investigate numerically, as a particular kind of elastic dipole-vortex interaction, the interaction between a translating eddy-pair and an axisymmetrical cyclonic eddy.

In view of the complexity of baroclinic three-dimensional (3D) vortices, it is more practical to investigate first the barotropic two-dimensional (2D) case, assuming an adiabatic, inviscid, and incompressible fluid, satisfying the Euler equation of motion, which in this case reduces to the material conservation of vertical vorticity $\zeta(\mathbf{x}, t) \equiv \mathbf{k} \cdot \nabla \times \mathbf{u}(\mathbf{x}, t)$, where $\mathbf{u}(\mathbf{x}, t)$ is the horizontal velocity field, ∇ is the 2D gradient operator and $\mathbf{k}$ is the vertical unit vector. Many geophysical processes occur on approximately horizontal scales, where the vertical, gravity oriented, velocity component is several orders of magnitude smaller than the horizontal velocity component (Wayne, 2011). For example, in the case of dipole-dipole interactions, Dubosq and Viúdez (2007) investigated numerically non-axial frontal collisions of mesoscale baroclinic eddy-pairs as well as 2D eddy-pair collisions, and concluded that the 3D inelastic interaction processes were qualitatively similar to the 2D interactions, as long as, the eddies had a similar vertical extent. In this study, where we deal with elastic interactions, the 2D processes are expected to be dominant. Nevertheless, we took a step forward and explored similar elastic interactions under the quasi-geostrophic (QG) 3D approximation of balanced, that is in absence of inertia–gravity waves, flows. In the QG balanced geophysical flows the geopotential $\phi(\mathbf{x}, t)$, horizontal geostrophic velocity $\mathbf{u}_h^g(\mathbf{x}, t) \equiv \mathbf{k} \times \nabla \phi(\mathbf{x}, t)$ and the materially conserved QG potential vorticity anomaly $\varpi^q(\mathbf{x}, t) = \nabla^2 \phi(\mathbf{x}, t)$, in the QG 3D space, is equivalent to the role played by the stream function $\psi(\mathbf{x}_h, t)$, horizontal velocity $\mathbf{u}_h(\mathbf{x}_h, t) \equiv \mathbf{k} \times \nabla \psi(\mathbf{x}_h, t)$ and the materially conserved vertical vorticity $\zeta(\mathbf{x}_h, t) = \nabla^2 \psi(\mathbf{x}_h, t)$ in the 2D isochoric flows.

The basic fluid dynamic equations for the 2D model, leading to the material conservation of vertical vorticity, are briefly introduced in section 2, while the basic QG equations are introduced in section 3. In the following section 4, the initial vorticity conditions are explained for the 2D case. The eddy-pair used is based on the Lamb-Chaplygin dipole (Chaplygin, 2007), which is an exact theoretical dipole model that translates rigid and straight with constant speed. The target axisymmetric cyclonic eddy has a radial vorticity distribution given by the Bessel function of 0-order $J_0(r)$. The initial conditions for the 3D dynamics are given in section 5. In the next step, section 6, we describe numerical results showing that the eddy-pair may be scattered by other ocean eddies, changing drastically its direction without modifying its vorticity distribution significantly, making therefore possible elastic interactions. The 3D simulations show similar results to the 2D cases, validating thus the more practical 2D model to describe barotropic mesoscale processes in adiabatic, inviscid and incompressible fluid and satisfying the Euler equation of motion. Finally concluding remarks are given in section 7.

2 Basic 2D Equations

In 2D isochoric flows the stream function $\psi(\mathbf{x}, t)$ provides the horizontal velocity $\mathbf{u}(\mathbf{x}, t)$,

$$\mathbf{u} \equiv -\nabla \times (\psi \mathbf{k}), \tag{1}$$

and vertical vorticity $\zeta(\mathbf{x}, t)$

$$\zeta \equiv \mathbf{k} \cdot \nabla \times \mathbf{u} = \nabla^2 \psi, \tag{2}$$

where $\mathbf{k}$ is the vertical unit vector and ∇ is the 2D gradient operator. The basic dynamical equation is the material conservation of vorticity

$$\frac{d\zeta}{dt} \equiv \frac{\partial \zeta}{\partial t} + \mathbf{u} \cdot \nabla \zeta = 0. \tag{3}$$

Equation (3) is numerically integrated (a brief description is given in Appendix A) to evolve in time the vorticity field from prescribed initial vorticity conditions $\zeta(\mathbf{x}, t_0)$. The results of these numerical simulations are described in section 6.

3 Basic QG 3D Equations

The inviscid adiabatic QG flow is governed, in a way similar to ζ in (3), by the conservation of QG potential vorticity anomaly (PVA) $\varpi^q(\mathbf{x}, t)$, as advected by the horizontal geostrophic flow

$$\frac{d\varpi^q}{dt} \equiv \frac{\partial \varpi^q}{\partial t} + \mathbf{u}_h^g \cdot \nabla_h \varpi^q = 0, \tag{4}$$

where $\mathbf{u}_h^g(\mathbf{x}, t) \equiv -\nabla \times (\phi \mathbf{e}_z)$, is the geostrophic velocity scaled by f_0^{-1}, where f_0 is the constant background planetary vorticity, or Coriolis parameter, and $\phi(\mathbf{x}, t)$ is the geopotential anomaly field. The QG PVA $\varpi^q(\mathbf{x}, t)$ is the sum of the dimensionless (scaled by f_0^{-1}) vertical component of geostrophic vorticity $\zeta^g(\mathbf{x}, t) = \nabla_h^2 \phi$ and the dimensionless vertical stratification anomaly $S(\mathbf{x}, t) = \partial D(\mathbf{x}, t)/\partial z = \partial^2 \phi/\partial \hat{z}^2$, where D is the vertical displacement of isopycnals, $\hat{z} \equiv (N_0/f_0)z$, and N_0 is the constant background Brunt–Väisälä frequency. The QG PVA $\varpi^q(\mathbf{x}, t)$

$$\varpi^q \equiv \zeta^g + S = \hat{\nabla}^2 \phi \tag{5}$$

equals, in the vertically stretched QG space $(x, y, \hat{z})$, the Laplacian of the geopotential anomaly $\phi(\mathbf{x}, t)$.

4 Initial Conditions for the 2D Model: Eddy-Pair and Axisymmetrical Cyclonic Eddy

To describe the eddy-pair, we use the Lamb-Chaplygin dipole model whose vorticity distribution $\zeta_d(r, \theta)$ in polar coordinates (r, θ) is a piecewise function given by

$$\zeta_d(r, \theta) \equiv \begin{cases} C_d \mathrm{J}_1(k_1 r) \sin \theta & 0 \leq k_1 r \leq j_{1,1} \\ 0 & j_{1,1} < k_1 r \end{cases}, \tag{6}$$

where C_d is a constant vorticity amplitude, $\mathrm{J}_m(r)$ is the Bessel radial of order m, $j_{m,n}$ is the nth zero of $\mathrm{J}_m(r)$ (Figure 1) and k_1 is the dipole's wavenumber. The interior and exterior velocity fields $\mathbf{u}_d(r, \theta)$, in polar coordinates, are given by

$$\frac{\mathbf{u}_d(r, \theta)}{C_d/k_1} \equiv \begin{cases} \frac{\mathrm{J}_1(k_1 r)}{k_1 r} \cos \theta \, \mathbf{e}_r - \frac{1}{2} \left(\mathrm{J}_0(k_1 r) - \mathrm{J}_2(k_1 r) \right) \sin \theta \, \mathbf{e}_\theta & 0 \leq k_1 r \leq j_{1,1} \\ \\ \frac{\mathrm{J}_0(j_{1,1})}{2k_1^2 r^2} \left[(k_1^2 r^2 - j_{1,1}^2) \cos \theta \, \mathbf{e}_r - (k_1^2 r^2 + j_{1,1}^2) \sin \theta \, \mathbf{e}_\theta \right] & j_{1,1} < k_1 r \end{cases}, \tag{7}$$

where $\mathbf{e}_r$ and $\mathbf{e}_\theta$ are the radial and azimuthal unit basis vectors, respectively.
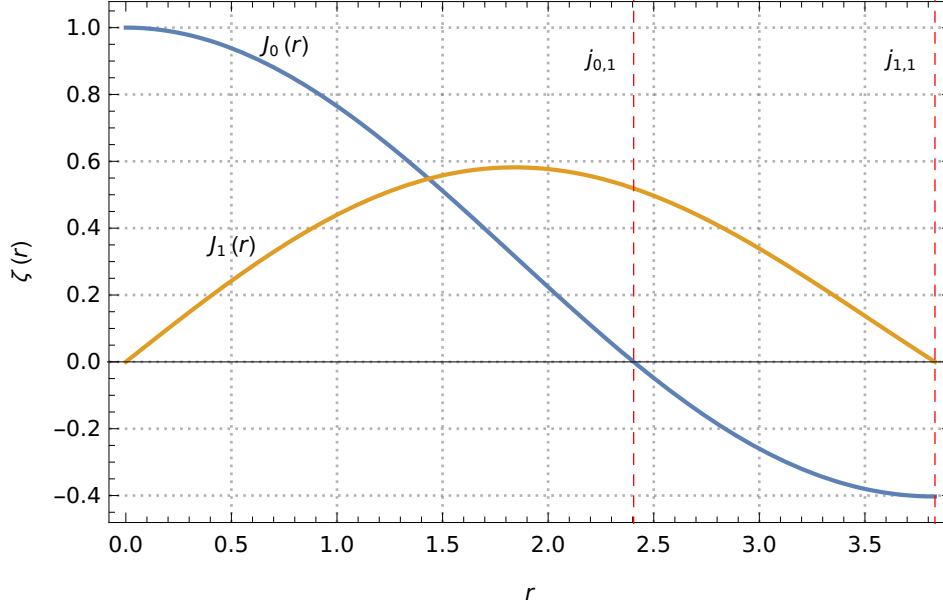
Figure 1. Bessel functions $J_0(r)$ (blue) and $J_1(r)$ (yellow). The red line stands for the zeroes $j_{0,1}$ and $j_{1,1}$

In order to provide flow solutions with vanishing velocity at infinity we must add to the steady piecewise flow (7) a background flow $\mathbf{u}_0(\mathbf{x}) \equiv -\mathbf{u}_d(\mathbf{r} \to \infty, \theta)$, applied to the complete spatial domain, such that the new time dependent velocity $\bar{\mathbf{u}}_d(r, \theta, t) \to \mathbf{0}$ as $r \to \infty$. The new solutions are time dependent and in Cartesian coordinates (x, y) are

$$\bar{\mathbf{u}}_d(x, y, t) \equiv \mathbf{u}_d(r(x - u_0 t, y), \theta(x - u_0 t, y)) + u_0 \mathbf{x}, \tag{8}$$

where $\mathbf{u}_d(r, \theta)$ is the velocity field (7) in the steady state, $r(x, y) = \sqrt{x^2 + y^2}$ and $\theta(x, y) = \arctan(y/x)$. Thus, the eddy-pair moves, in absence of background velocity, straight along the x-axis with a constant speed equal to $u_0 = -C_d J_0(j_{1,1})/(2k_1)$.

The vorticity distribution $\zeta_v(r, \theta)$ of the axisymmetrical cyclonic eddy is given by the Bessel function of order 0 (Figure 1), truncated at a radius $r = j_{0,1}/k_2$, that is

$$\zeta_v(r, \theta) \equiv \begin{cases} C_v J_0(k_2 r) & 0 \leq k_2 r \leq j_{0,1} \\ 0 & j_{0,1} < k_2 r \end{cases}, \tag{9}$$

where C_v is a constant vorticity amplitude and k_2 is the cyclone's wavenumber. The velocity of the cyclonic eddy $\mathbf{u}_v(r) = v(r)\mathbf{e}_\theta$ is azimuthal and is given by

$$\frac{v(r)}{C_v/k_2} \equiv \begin{cases} J_1(k_2 r) & 0 \leq k_2 r \leq j_{0,1} \\ \frac{J_1(j_{0,1})j_{0,1}}{k_2 r} & j_{0,1} < k_2 r \end{cases}. \tag{10}$$

When both, the eddy-pair and the axisymmetrical cyclonic eddy, are present they interact due to their exterior potential flows. This interaction depends on the vortices amplitudes (C_d, C_v) and vortices extension given by the wavenumbers (k_1, k_2). Since we are interested in interactions between vortices with equal size and amplitude we therefore set the positive circulation of the eddy-pair (Γ_d^+) equal to the circulation of the axisymmetrical cyclonic eddy (Γ_v^+), and the area of the target eddy (A_v) equal to the area of the positive vorticity of the eddy-pair (A_d^+), that is,

$$\Gamma_d^+ = \Gamma_v^+, \quad A_d^+ = A_v. \tag{11}$$

The radius of the target cyclonic eddy is $R_v = j_{0,1}/k_2$, which implies $A_v = \pi(j_{0,1}/k_2)^2$. Since the radius of the eddy-pair is $R_d = j_{1,1}/k_1$, the area is $A_d^+ = \pi(j_{1,1}/k_1)^2/2$ and applying (11), we obtain the wavenumber ratio

$$\frac{k_1}{k_2} = \frac{1}{\sqrt{2}} \frac{j_{1,1}}{j_{0,1}} \simeq 1.127 \,. \tag{12}$$

The amplitudes ratio C_v/C_d is obtained equating the circulation of the target eddy to the positive circulation of the eddy-pair. The positive circulation of the eddy-pair is

$$\frac{\Gamma_d^+}{C_d} = \int_0^\pi \sin\theta \, d\theta \int_0^{j_{1,1}/k_1} \mathrm{J}_1(k_1 r) \, r \, dr = -\frac{\pi}{k_1^2} j_{1,1} \mathrm{H}_1(j_{1,1}) \mathrm{J}_0(j_{1,1}) \,, \tag{13}$$

where $\mathrm{H}_1(x)$ is the Struve function of order 1. This is consistent with the circulation of one-half of the Lamb dipole obtained by (Kloosterziel et al., 1993). The circulation of the axisymmetrical eddy is

$$\frac{\Gamma_v^+}{C_v} = \int_0^{2\pi} d\theta \int_0^{j_{0,1}/k_2} \mathrm{J}_0(k_2 r) \, r \, dr = \frac{2\pi}{k_2^2} j_{0,1} \mathrm{J}_1(j_{0,1}) \,, \tag{14}$$

and therefore applying (11) we obtain the vorticity amplitudes ratio

$$\frac{C_d}{C_v} = -\frac{j_{1,1} \mathrm{J}_1(j_{0,1})}{\mathrm{H}_1(j_{1,1}) \mathrm{J}_0(j_{1,1}) j_{0,1}} \simeq 1.889 \,. \tag{15}$$

The initial vorticity distribution is represented in figure 2. The eddy-pair's poles are close together and have the same vorticity contours as the axisymmetrical eddy. The initial interaction between both vortices, as inferred from the stream function is negligible. This initial vorticity distribution is integrated in time following the steps explained in Appendix A and the results are described in section 6.

5 Initial Conditions for the QG 3D Model: Eddy-Pair and Axisymmetrical Cyclonic Eddy

In the 3D geophysical QG approach, instead of the cylindrical Bessel functions of the first kind $\mathrm{J}_n(r)$, which are the eigenfunctions of the radial part of the Laplacian operator in polar coordinates (r, θ), the relevant modes are the spherical Bessel functions of the first kind $\mathrm{j}_l(\rho)$ and the spherical harmonics $\mathrm{Y}_l^m(\vartheta, \varphi)$, of degree l and order m, which are the eigenfunctions of the radial part (ρ) and the angular part (ϑ, φ), respectively, of the Laplacian operator in spherical coordinates $(\rho, \vartheta, \varphi)$. Also in 3D, the Lamb-Chaplygin dipole model is used to decribe the eddy-pair. The QG PVA of the dipole ϖ_d^q is a piecewise function given by

$$\varpi_d^q(\rho, \vartheta, \varphi) \equiv \begin{cases} -B_d \, \mathrm{j}_1(k_d \rho) \sin\vartheta \cos\varphi & 0 \le k_d \rho \le j_{\frac{3}{2},1} \\ 0 & j_{\frac{3}{2},1} < k_d \rho \end{cases} \,, \tag{16}$$

where B_d is a constant potential vorticity anomaly amplitude of the dipole and k_d is the dipole's wavenumber. The piecewise function of the PVA of the axisymmetrical cyclonic eddy in the QG space is given by

$$\varpi_v^q(\rho, \vartheta, \varphi) \equiv \begin{cases} -B_v \, \mathrm{j}_0(k_v \rho) & 0 \le k_v \rho \le j_{\frac{1}{2},1} \\ 0 & j_{\frac{1}{2},1} < k_v \rho \end{cases} \,, \tag{17}$$

where B_v is the constant amplitude and k_v is the wavenumber of the cyclone. As it happens in the 2D case, the interaction depends on the vortices amplitudes (B_d, B_v) and extension given by the wavenumbers (k_d, k_v). Since we want to investigate in 3D
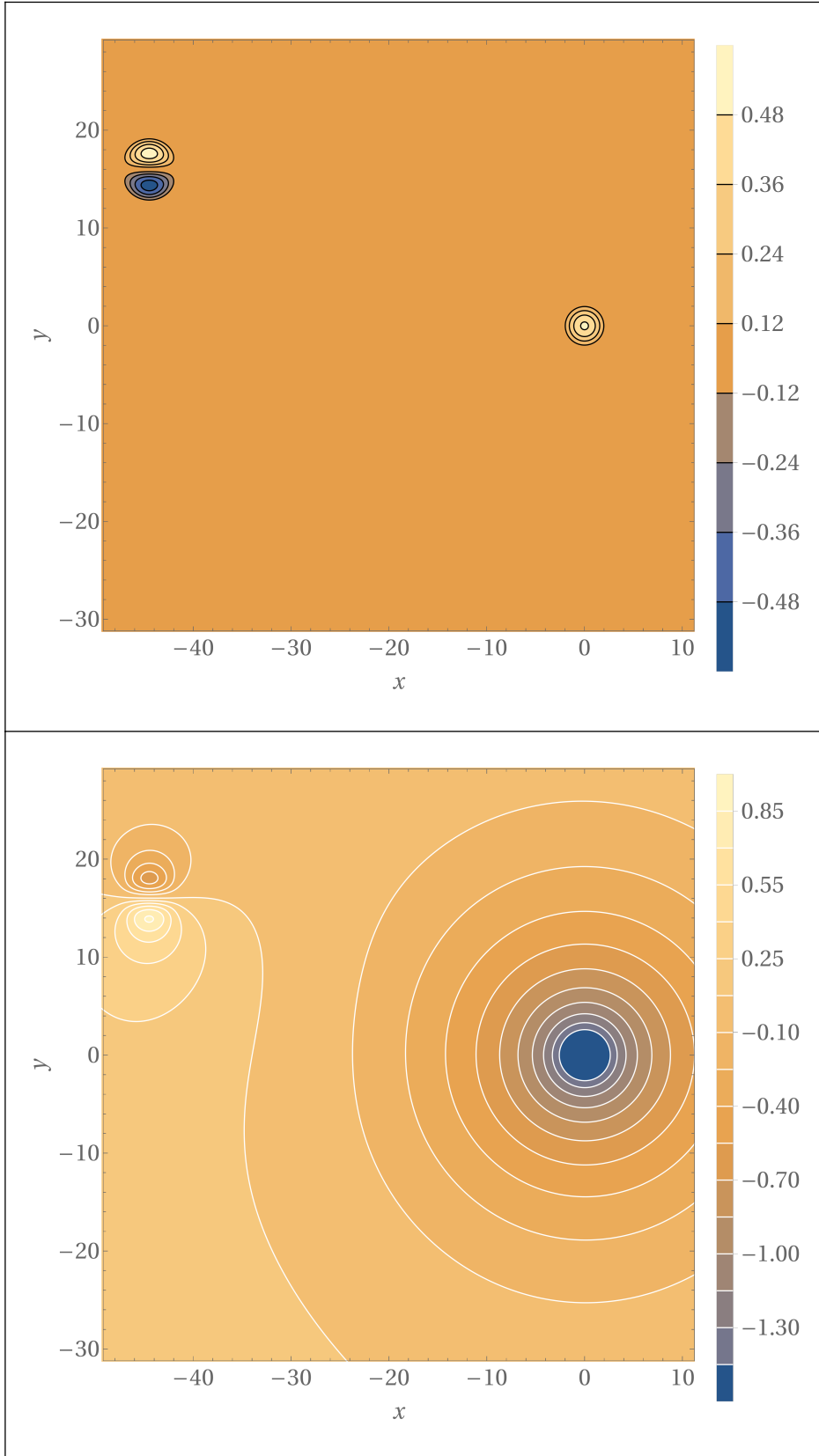
Figure 2. Vorticity (top) and stream function (bottom) distributions at $t = 0$.

QG flows the baroclinic effects of elastic interactions we apply (11), where instead of the integrated area, now volume integration applies

$$\hat{\Gamma}_d^+ = \hat{\Gamma}_v^+ \,, \quad V_d^+ = V_v \,. \tag{18}$$

The volume of the cyclonic eddy of the eddy-pair is $V_d^+ = 2\pi R_d^3/3$, where R_d is the boundary radius of the eddy-pair. While the positive circulation of the eddy-pair in the QG space is

$$
\begin{aligned}
\frac{\hat{\Gamma}_d^+}{B_d} &= \int_{-\pi/2}^{\pi/2} \cos\varphi\, d\varphi \int_0^\pi (\sin\vartheta)^2\, d\vartheta \int_0^{R_d} \mathrm{j}_1(k_d\rho)\, \rho^2\, d\rho \\
&= -\frac{2\pi((k_d^2 R_d^2 + 2)\mathrm{j}_0(k_d R_d) - 2(k_d R_d \mathrm{j}_1(k_d R_d) + 1))}{3k_d^3} \,.
\end{aligned}
\tag{19}
$$

The volume of the target axisymmetrical eddy is $V_v = 4\pi R_v^3/3$, where R_v is the radius boundary of the cyclone and the circulation of the cyclone is

$$\frac{\hat{\Gamma}_v^+}{B_v} = \int_0^{2\pi} d\varphi \int_0^\pi \sin\vartheta \int_0^{R_v} \mathrm{j}_0(k_v\rho)\, \rho^2\, d\rho = \frac{4\pi R_v^2 \mathrm{j}_1(k_v R_v)}{k_v} \,. \tag{20}$$

From (18) we obtain the wavenumbers ratio

$$\frac{k_d}{k_v} = \frac{\mathrm{j}_1(1)}{2^{1/3}\pi} \simeq 1.135 \tag{21}$$

and the amplitudes ratio

$$\frac{B_d}{B_v} \simeq 4.043. \tag{22}$$

This approach has been used recently to investigate three-dimensional baroclinic dipoles (Viúdez, 2019). In the next section, we describe the numerical results of the elastic interaction between the Eddies.

6 Numerical Results

In order to describe the numerical results we define the time dependent center positions of the positive and negative vorticity parts of the 2D eddy-pair ($\mathbf{r}_d^+(t)$ and $\mathbf{r}_d^-(t)$, respectively),

$$\mathbf{r}_d^\pm(t) \equiv \frac{\int_{A_d^\pm}(x,y)\, \tilde{\zeta}(x,y,t)\, dx\, dy}{\int_{A_d^\pm} \tilde{\zeta}(x,y,t)\, dx\, dy} \,, \tag{23}$$

where $A_d^\pm$ are the time dependent regions of points (x,y,t) where $\pm\tilde{\zeta}(x,y,t) > 0$. The time dependent center of the eddy-pair $\mathbf{r}_d$ is given by

$$\mathbf{r}_d(t) \equiv \frac{\mathbf{r}_d^+(t) + \mathbf{r}_d^-(t)}{2} \,. \tag{24}$$

The time dependent center position of the axisymmetrical eddy $\mathbf{r}_v(t)$ is defined in an analogous way to (23).

Initially the eddy-pair moves with an almost straight trajectory approaching the axisymmetrical cyclonic eddy (Figure 3). As the eddy-pair gets closer to the target eddy, the dipole-vortex interaction increases due to the potential background-flows of both vortical structures. As a result of this interaction the eddy-pair is attracted by the axisymmetrical cyclonic eddy and its trajectory acquires negative curvature (Figure 3). On the other hand, the axisymmetrical eddy is also attracted by the eddy-pair's potential-flow, and is slightly accelerated towards the approaching eddy-pair (Figure 3). The closer the vortices get, the eddy-pair's speed of displacement decreases (Figure 4) due to the fact that the eddy-pairs poles open up relative to the
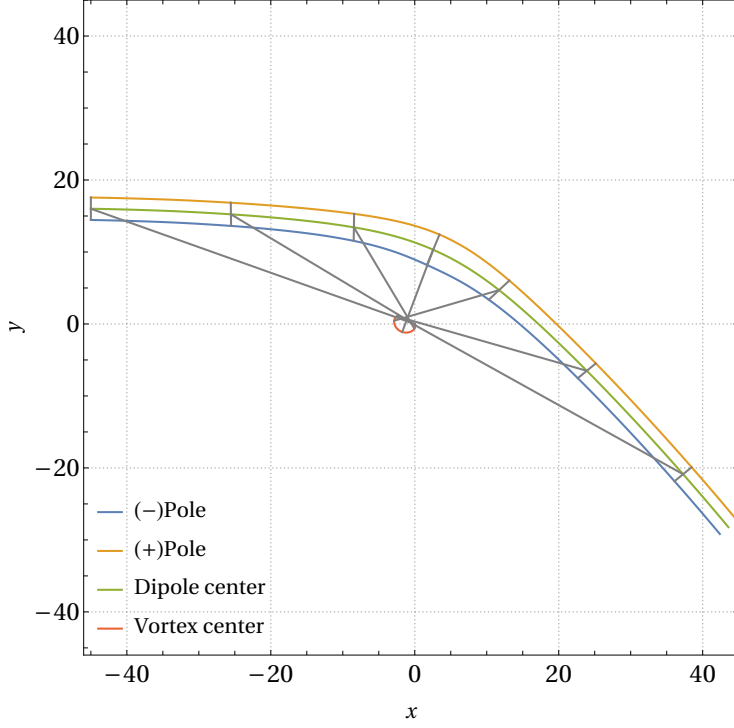
Figure 3. Trajectories of the center of the eddy-pair poles $\mathbf{r}^-(t)$ (blue), $\mathbf{r}^+(t)$ (orange), the center of the eddy-pair $\mathbf{r}_d(t)$ (green), and the center of the axisymmetrical cyclonic eddy $\mathbf{r}_v(t)$ (red) for the 2D case. The gray lines connect the $+$ and $-$ pole centers and the center of the eddy-pair with the center of the target cyclonic eddy at seven different times.
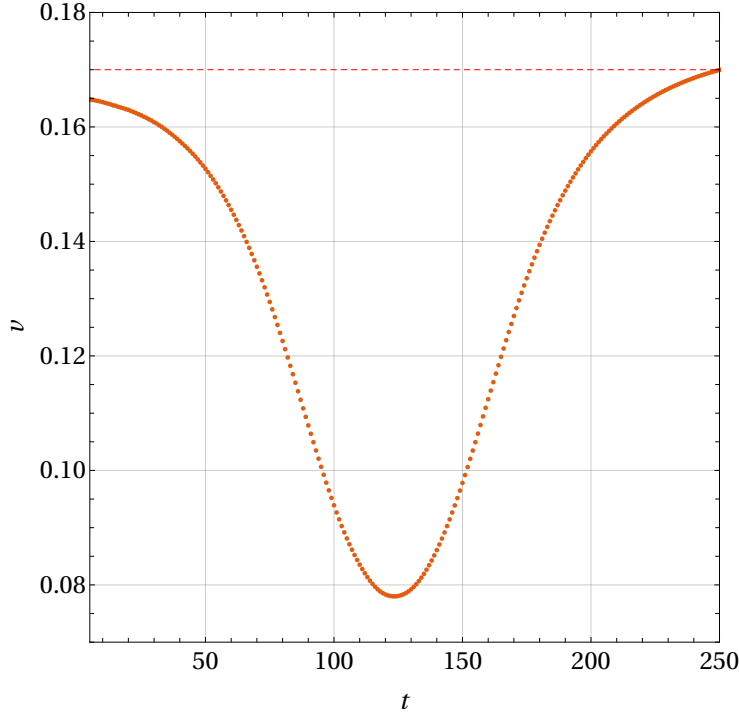

Figure 4. Speed of displacement $v_d(t) \equiv |d\mathbf{r}_d(t)/dt|$ of the eddy-pair for the 2D case. The dashed red line marks the speed of displacement of the last point.
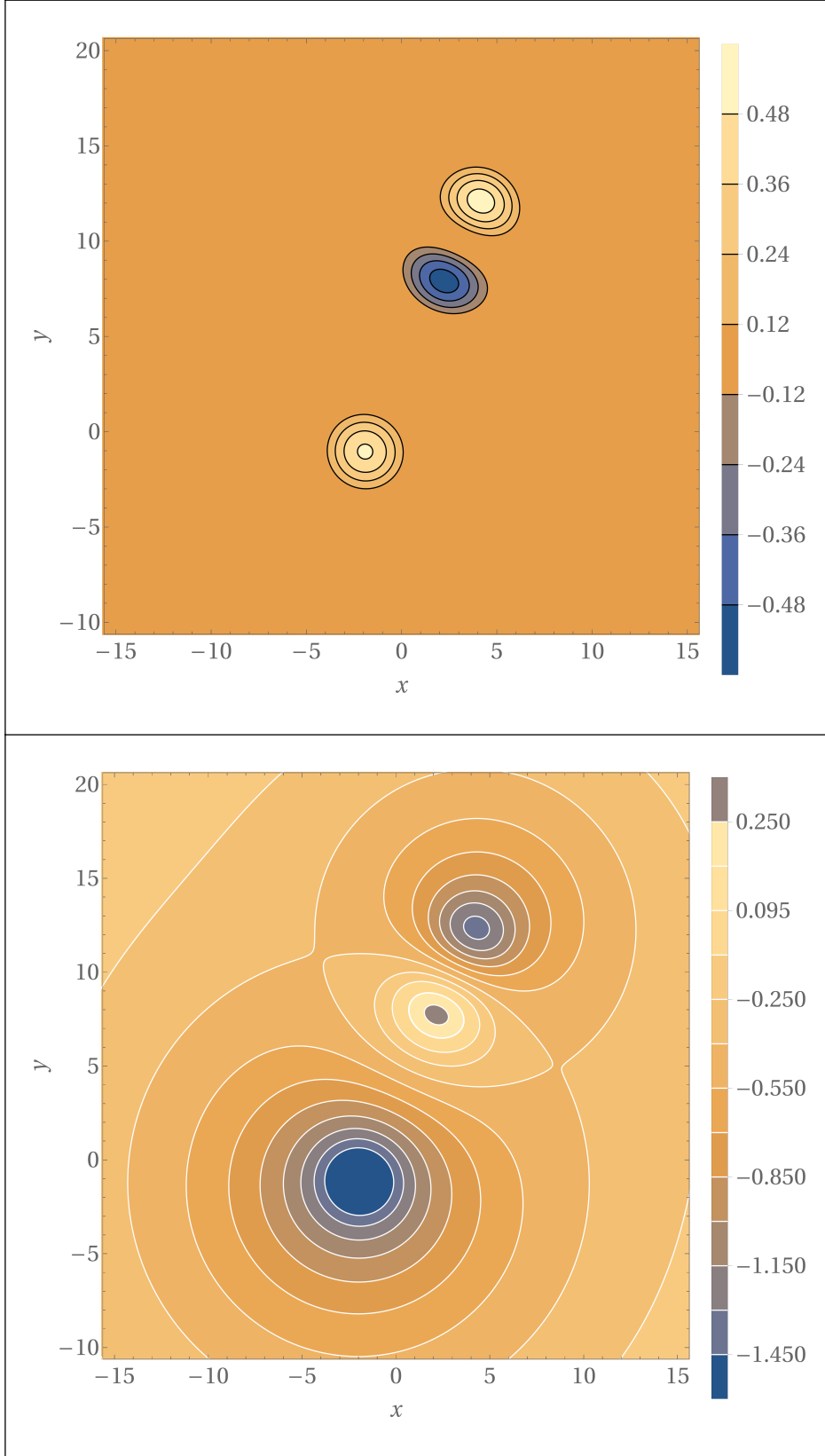
Figure 5. Vorticity (top) and stream function (bottom) distributions at the time of maximum poles separation ($t = 123$) for the 2D case.

eddy-pair's axis (Figures 3 and 5). At the time of highest pole separation ($t \simeq 123$) the eddy-pair's speed of displacement reaches a minimum (Figure 4) and the two centers of the vortices, as well as the centers of the poles, are completely aligned (Figure 3).

In this case, due to the large North-South initial distance between the eddy-pair and the axisymmetrical cyclonic eddy, there is no vorticity exchange between the vortices. After the time of largest interaction ($t \simeq 123$, Figure 5), the poles of the eddy-pair close and the eddy-pair acquires a rigid vorticity distribution which is similar to its initial one but rotated positively (Figure 3).

The mechanism of the eddy-pair's trajectory change, due to the interaction between the potential flows, involves a very small exchange of vorticity between the positive and negative poles and also a small vorticity leakage, of both positive and negative vorticity, to the background field. While a Lamb-Chaplygin dipole consisting only of the first vorticity mode $J_1(k_1 r)$, dipolar antisymmetrical mode, moves along a straight trajectory, the presence of the zero-mode $J_0(k_2 r)$, or rotational symmetrical mode, provides a constant curvature to the trajectory of the eddy-pair. In this numerical experiment the eddy-pair, consisting initially of only the first vorticity mode $J_1(k_1 r)$, develops a small rotational mode via vorticity exchange between the poles while approaching the axisymmetrical cyclonic eddy. The direction of this vorticity exchange is reversed as the eddy-pair leaves the target eddy, in such a way that the mode-0 vanishes and the poles recover their antisymmetrical vorticity distribution. On the other side, the axisymmetrical cyclonic eddy decelerates towards a new position very close to its initial location (Figure 3). The same interaction occurs in the 3D QG approximation with barotropic effects. At the beginning of the simulation, the axisymmetrical eddy is spherical and both circulation parts of the eddy-pair have an ellipsoidal antisymmetric geometry, while they translate straight forward approaching the rotating axisymmetrical eddy (Figure 6). When the eddy-pair approaches the axisymmetrical cyclonic eddy, the eddy-pair changes its trajectory and geometry, losing its initial vorticity antisymmetry. The negative vorticity isosurfaces form larger ellipsoids, while the positive vorticity isosurfaces acquire an almost spherical geometry (Figure 6). The axisymmetrical vortex which originally is a rotating sphere, in presence of the first spherical Bessel mode (j_1) suffers a small displacement and acquires an ellipsoidal geometry reaching its maximum deformation at the highest interaction ($t \simeq 45$) (Figure 6). After the interaction the vortices return to its original geometry, with different position and displacement direction in the case of the eddy-pair similar to the 2D case. The whole interaction process is shown for the 2D and 3D cases in the videos referenced in Figure 7 and Figure 8. Since the 2D and the 3D cases show similar results, for the initial conditions given here, we describe with more detail the interaction in 2D.

The eddy-pair's speed of displacement after the interaction is very close to its original value (Figure 4). This interaction, practically involving no net vorticity change between initial and final eddy-pair vorticity distributions, may be classified as an elastic scattering of an eddy-pair by an axisymmetrical eddy. Nevertheless, it is important to underline that changes in the initial vorticity distribution of the axisymmetrical cyclonic eddy this interaction may lose its elastic behaviour. For example, if the axisymmetrical eddy vorticity boundary R_v is extended to the first zero $j_{1,1}/k_2$, in such a way that the cyclonic eddy vorticity distribution is $\zeta(r)/C_v = J_0(k_2 r) - J_0(j_{1,1})$, so that there is no vorticity jump at the eddy boundary $\zeta(j_{1,1}/k_2) = 0$, the interaction is fully inelastic. In this case it occurs an exchange of the negative vorticity pole between the eddy-pair and the axisymmetrical eddy. This example is described in more detail in Appendix B. Furthermore, if the amplitude of the axisymmetrical eddy is large enough, its potential flow may break the approaching eddy-pair even before any vorticity interaction can take place.
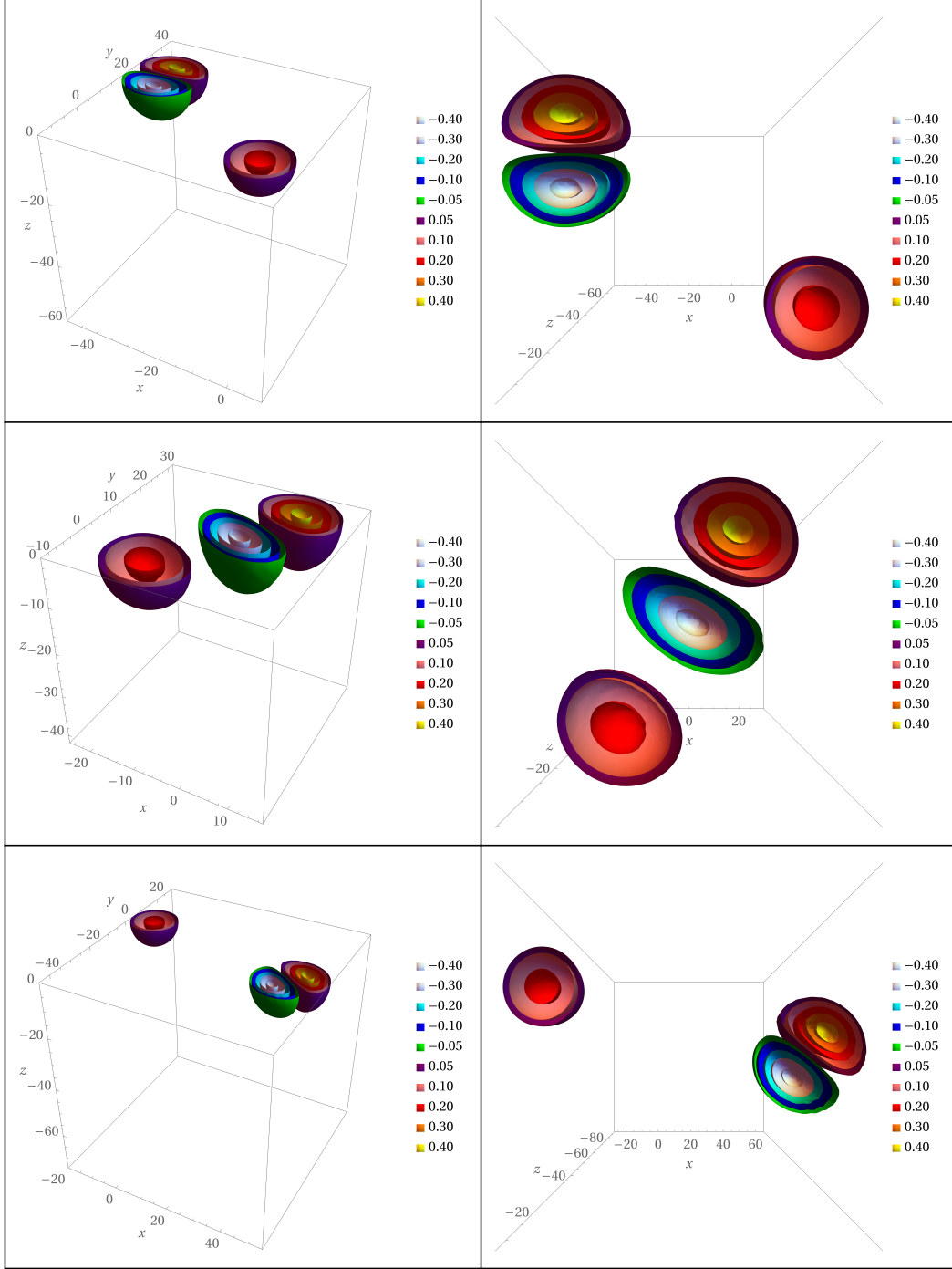
Figure 6. Potential vorticity anomaly distribution at the beginning of the simulation ($t = 15$, top), at the time of maximum poles separation ($t = 45$, middle) and close to the end of the simulation ($t = 75$, bottom) for the 3D geophysical flow under the quasi-geostrophic approximation. Point of view Top-down (left) and from the z-axis (right).
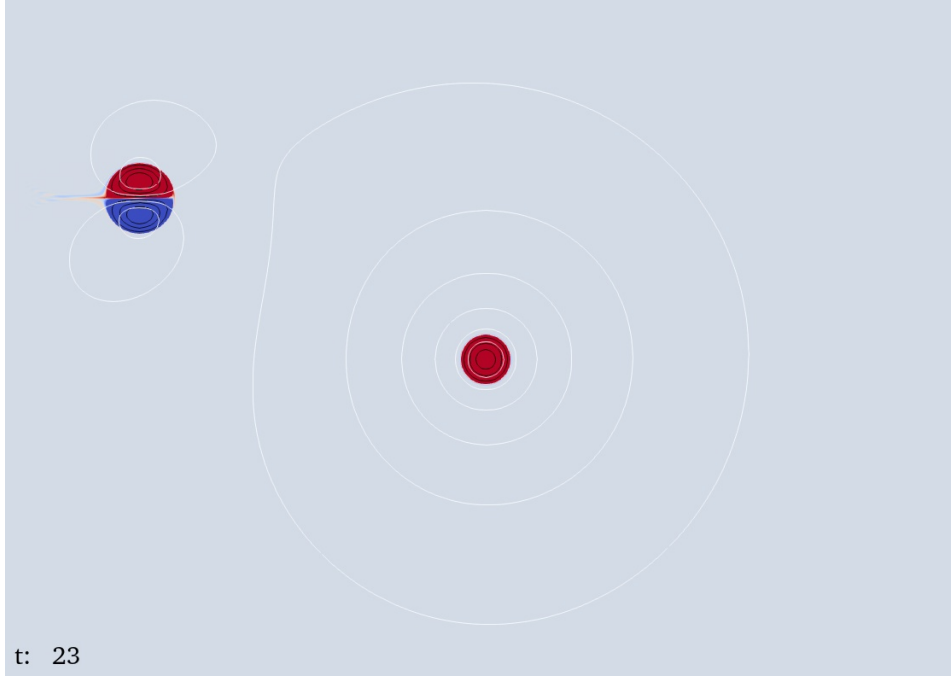
Figure 7. Video of the elastic interaction between the eddy-pair and the axisymmetrical cyclonic eddy in isochoric two-dimensional flows. The colour scale is saturated for a better visualization of the small vorticity changes. Blue and red colors mean negative and positive vorticity, respectively. Vorticity contour lines (black) and stream function contour lines (white) are included.
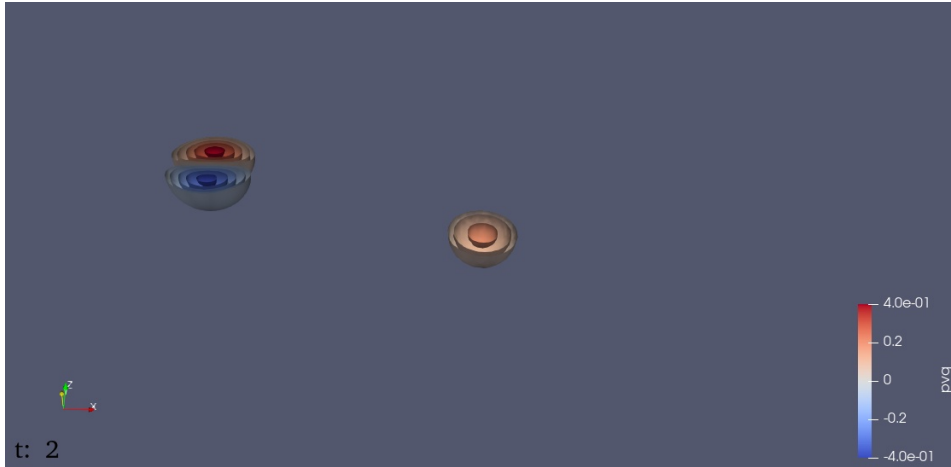

Figure 8. Video of the elastic interaction between the eddy-pair and the axisymmetrical cyclonic eddy in the quasi-geostrophic three-dimensional space. Blue and red colors mean negative and positive potential vorticity anomaly (PVA), respectively.
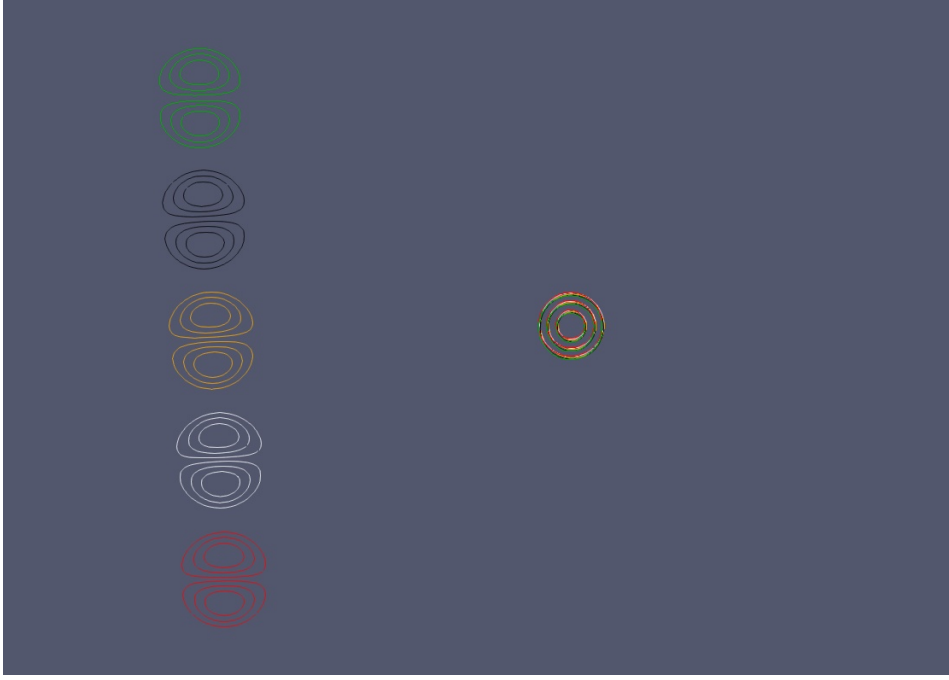
Figure 9. Video of the superposition of five different simulations, represented with different vorticity contour line colors, of the interaction between the eddy-pair and the axisymmetrical cyclonic eddy. Each eddy-pair starts at a different y-axis position. The axisymmetrical eddy is always placed at the position $(0,0)$.

We have also analyzed 2D interactions similar to the one described before but changing the initial positions of the eddy-pair along the y-axis (video referenced in Figure 9). In this video, the eddy-pair with green vorticity contours at the top simulates the elastic interaction described above. The eddy-pair with black vorticity contours is located half the way of the green eddy-pair. This interaction is really similar to the interaction described in Appendix B where the eddy-pair is scattered by the axisymmetrical eddy and the eddy-pair's poles separate. When the negative pole is close to the positive axisymmetrical eddy, these two vortices join together, giving rise to partner exchange and formation of a new eddy-pair (video in Figure 9). The positive vorticity pole of the eddy-pair is left behind and evolves towards an axisymmetrical cyclonic eddy close to the initial position of the initial axisymmetrical cyclonic eddy.

The next eddy-pair, with yellow vorticity contours, is located at the same y-coordinate as the axisymmetrical cyclonic eddy ($y = 0$). In this case, the vortices collide and merging occurs (video in Figure 9). The next two eddy-pairs, with white and red vorticity contours, are situated at the same distance as the vortices black and green, respectively, but with reversed sign, so that the positive pole of the eddy-pair is the closest pole to the axisymmetrical cyclonic eddy. In these cases, a positive-positive pole interaction occurs. The white eddy-pair, closer to the axisymmetrical cyclonic eddy, suffers straining out vorticity processes, while the red eddy-pair, far from the axisymmetrical eddy, experiences also an elastic interaction but weaker than the one experienced by the green eddy-pair (video in Figure 9). In this case, the red eddy-pair is slightly repelled, instead of being attracted, by the axisymmetrical eddy, in such a way that the eddy-pair changes only slightly its direction during the interaction time, to afterwards return to a straight trajectory with the same initial direction. The axisymmetrical eddy behaves similar to the eddy-pair, it is repelled by the potential
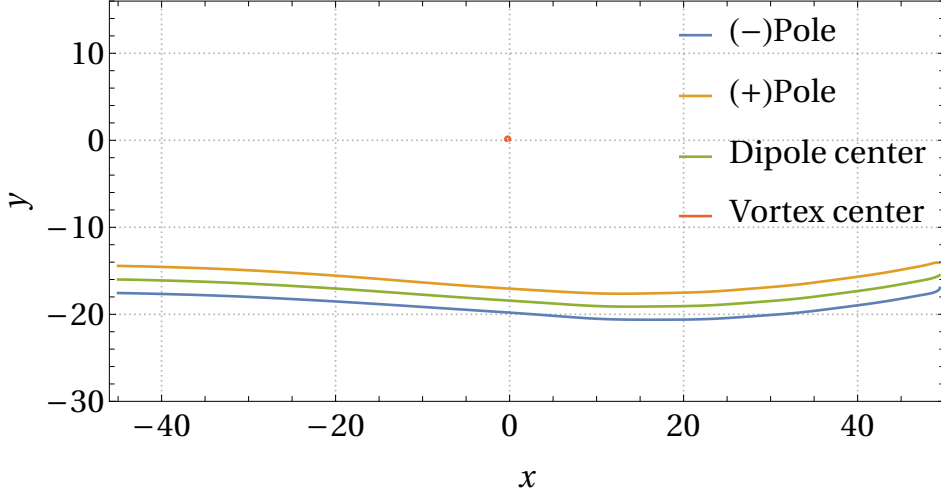
Figure 10. Trajectories of the center of the eddy-pair poles $\mathbf{r}^-(t)$ (blue), $\mathbf{r}^+(t)$ (orange), the center of the eddy-pair $\mathbf{r}_d(t)$ (green), and the center of the axisymmetrical eddy $\mathbf{r}_v(t)$ (red).

flow of the eddy-pair and describes an almost semi-circular trajectory with a small radius $\delta r \simeq 0.6$ (too small to be appreciated in Figure 10) and returns, after the interaction time, to a new location very close to the initial one.

7 Concluding Remarks

In this work we have proved, using numerical simulations, that fully elastic interactions between a mesoscale eddy-pair and an axisymmetrical eddy are possible in three-dimensional geophysical flows. The elastic interactions described here occur in inviscid incompressible flows, both under the three-dimensional quasi-geostrophic approximation, where the potential vorticity anomaly is materially conserved, and in two-dimensional flows where the vertical vorticity is materially conserved. The results for the 2D and 3D cases show that interactions with almost no vorticity exchange or vorticity loss to the background field between ocean eddies are possible, changing the position and displacement direction of the eddies. In the particular example described in detail in this work, a Lamb-Chaplygin dipole (eddy-pair) is elastically scattered by an axisymmetrical cyclonic eddy. When the initially straight moving eddy-pair approaches the target cyclonic eddy they interact due to their corresponding potential flows. A barotropic effect of the interaction is that the trajectory of the eddy-pair acquires curvature and the eddy-pair's vorticity poles, formed by the anticyclonic and cyclonic eddy, separate from each other. Once the eddy-pair moves away from the target eddy, the anticyclonic and cyclonic eddy of the eddy-pair come closer again and the eddy-pair continues as a Lamb-Chaplygin dipole with a straight trajectory but with a direction different from the initial one. Under the QG approximation, little changes in the eddies occur along the vertical axis, and the barotropic effects are dominant. As the eddy-pair approaches the axisymmetrical eddy, the negative vorticity pole (anticyclone of the eddy-pair), which gets closer to the axisymmetrical cyclonic eddy, elongates horizontally while, simultaneously, the positive vorticity pole (cyclone of the eddy-pair) evolves towards spherical geometry and the axisymmetrical eddy acquires prolate ellipsoidal geometry. After the interaction both eddy structures return to their original geometry. No significant vorticity exchange between the eddy-pair and the axisymmetrical eddy occurs. Though there is a very small vorticity exchange

between the poles and a small vorticity leakage to the background field, the vortex interaction may be considered, from a practical point of view, as an elastic interaction.

This description of an elastic interaction contributes to several previous studies involving eddy-pair interactions, including interactions of dipoles with solid boundaries (de Ruijter et al., 2004; Kloosterziel et al., 1993; Voropayev & Afanasyev, 1992; Zavala Sansón & Gonzalez, 2021), interactions of dipoles with inertia–gravity waves (Claret & Viúdez, 2010; Huang et al., 2017), and dipole-dipole interactions (Dubosq & Viúdez, 2007; McWilliams & Zabusky, 1982; Velasco Fuentes & Heijst, van, 1995; Voropayev & Afanasyev, 1992). In the cases of dipole-dipole and dipole-vortex interactions both elastic and inelastic processes are possible depending on the initial vorticity distribution, which includes the location, orientation and vorticity distributions of the eddies. This work fills the gap of a detailed explanation of elastic interaction. In the main example shown in this work, due to the particular initial conditions chosen, inelastic interactions do not occur, and the interaction processes between eddies are practically elastic.

Our future work is to investigate the stability of neutral (that is, with vanishing amount of potential vorticity anomaly) geophysical vortices, including also eddy interactions, extending the approach of Viúdez (2021) in 2D to three-dimensional QG flows.

Appendix A Scheme of the Numerical Algorithm

Given an initial vorticity field $\zeta(x, y, t_0)$ the vorticity time integration is done in four steps.

1. The stream function $\psi(x, y, t_0)$ is obtained by solving (2) espectrally.
2. The velocity $\mathbf{u}(x, y, t_0)$ is computed from $\psi(x, y, t_0)$ using (1).
3. The vorticity advection $-\mathbf{u} \cdot \nabla \zeta$ is computed in the physical space.
4. The vorticity at the next time-step $\zeta(x, y, t_0 + \delta t)$ is obtained from (3) as

$$\zeta(x, y, t_0 + \delta t) = -\delta t\, \mathbf{u} \cdot \nabla \zeta + \zeta(x, y, t_0)\,.$$

After the step 4 the loop returns to step 1 for the next time integration $(t_0 + \delta t)$. The numerical simulations were carried out using a 2D pseudospectral code where the vorticity field $\zeta(x, y, t)$ is numerically integrated, following the steps described above, in a doubly periodic domain using an explicit leap-frog time-stepping method, together with a weak Robert-Asselin time filter to avoid the decoupling of even and odd time levels. The numerical domain was discretized in 2048^2 grid points.

Appendix B Dependence with the Radial Vorticity Profile of the Axisymmetrical Vortex

In this case the axisymmetrical eddy boundary R_v is extended to the first zero $R_v = j_{1,1}/k_2$, instead of $j_{0,1}/k_2$ (Figure 1), and its vorticity distribution is given by $\zeta(r)/C_v = J_0(k_2 r) - J_0(j_{1,1})$ so that $\zeta(j_{1,1}/k_2) = 0$ with no vorticity jump at the eddy boundary. The other initial conditions described in section 4 remain unchanged. In the general case where the eddy boundary is taken at $k_2 r = j_{m,n}$ the external flow $\mathbf{u}_0(r)$, is given by

$$\frac{\mathbf{u}_0(r)}{C_v/k_2} = \left[\frac{J_0(j_{m,n})}{2} \frac{j_{m,n}^2}{k_2 r} - J_1(j_{m,n}) \frac{j_{m,n}}{k_2 r} \right] \mathbf{e}_\theta\,.$$

If the eddy boundary is taken at $k_2 r = j_{1,1}$ the external flow decays as $C_v(J_0(j_{1,1}) j_{1,1}^2/(2 k_2^2 r)) \simeq -2.9/(k_2^2 r)$, while if the eddy boundary is taken at $k_2 r = j_{0,1}$, as in section 4,

the external flow decays as $-C_v(\mathrm{J}_1(j_{0,1})j_{0,1}/(k_2^2 r)) \simeq -1.2/(k_2^2 r)$, the ratio been $\mathrm{J}_0(j_{1,1})j_{1,1}^2/(2\mathrm{J}_1(j_{0,1})j_{0,1}) \simeq 2.4$, indicates that the external flow in this example decays faster than the exterior flow in section 4.

In this case, the eddy-pair moves initially with a straight trajectory approaching the axisymmetrical eddy. Then, the eddies are attracted by their potential flows and the eddies of the eddy-pair separate. The difference with the case studied in section 6 is that, in this case, while the eddies of the eddy-pair separate themselves from each other, the axisymmetrical cyclonic eddy is pushed away from the eddy-pair, and the anticyclone of the eddy-pair separates from the cyclone of the eddy-pair and joins the axisymmetrical cyclonic eddy, giving rise to a new eddy-pair (Figure B1). The cyclone of the original eddy-pair is left behind and remains as an axisymmetrical eddy close to the position of the original one.

Acknowledgments

References

Afanasyev, Y. (2003). Spontaneous emission of gravity waves by interacting vortex dipoles in a stratified fluid: Laboratory experiments. *Geophysical & Astrophysical Fluid Dynamics*, *97*(2), 79-95. doi: 10.1080/0309192031000114349

Ahlnäs, K., Royer, T. C., & George, T. H. (1987). Multiple dipole eddies in the Alaska Coastal Current detected with Landsat thematic mapper data. *Journal of Geophysical Research: Oceans*, *92*(C12), 13041-13047. doi: https://doi.org/10.1029/JC092iC12p13041

Barton, E. D., Arístegui, J., Tett, P., & Navarro-Pérez, E. (2004). Variability in the Canary Islands area of filament-eddy exchanges. *Progress in Oceanography*, *62*(2), 71-94. (The Canary Islands Coastal Transition Zone - Upwelling, Eddies and Filaments) doi: https://doi.org/10.1016/j.pocean.2004.07.003

Besse, V., Leblond, H., Mihalache, D., & Malomed, B. (2014). Building patterns by traveling dipoles and vortices in two-dimensional periodic dissipative media. *Optics Communications*, *332*, 279-291. doi: https://doi.org/10.1016/j.optcom.2014.07.029

Carton, X. (2001, 05). Hydrodynamical modeling of oceanic vortices. *Surveys in Geophysics*, *22*, 179-263. doi: 10.1023/A:1013779219578

Chaplygin, S. (2007, 04). One case of vortex motion in fluid. *Regul. Chaot. Dyn.*, *12*, 219-232. doi: 10.1134/S1560354707020074

Claret, M., & Viúdez, A. (2010, 12). Vertical velocity in the interaction between inertia–gravity waves and submesoscale baroclinic vortical structures. *Journal of Geophysical Research (Oceans)*, *115*, C12060. doi: 10.1029/2009JC005921

Couder, Y., & Basdevant, C. (1986, 12). Experimental and numerical study of vortex couples in two-dimensional flows. *Journal of Fluid Mechanics*, *173*, 225-251. doi: 10.1017/S0022112086001155

de Ruijter, W. P., van Aken, H. M., Beier, E. J., Lutjeharms, J. R., Matano, R. P., & Schouten, M. W. (2004). Eddies and dipoles around South Madagascar: formation, pathways and large-scale impact. *Deep Sea Research Part I: Oceanographic Research Papers*, *51*(3), 383-400. doi: https://doi.org/10.1016/j.dsr.2003.10.011

Dritschel, D. G. (1995). A general theory for two-dimensional vortex interactions. *Journal of Fluid Mechanics*, *293*, 269303. doi: 10.1017/S0022112095001716

Dritschel, D. G., & Waugh, D. W. (1992). Quantification of the inelastic interaction of unequal vortices in two-dimensional vortex dynamics. *Physics of Fluids*, *4*,
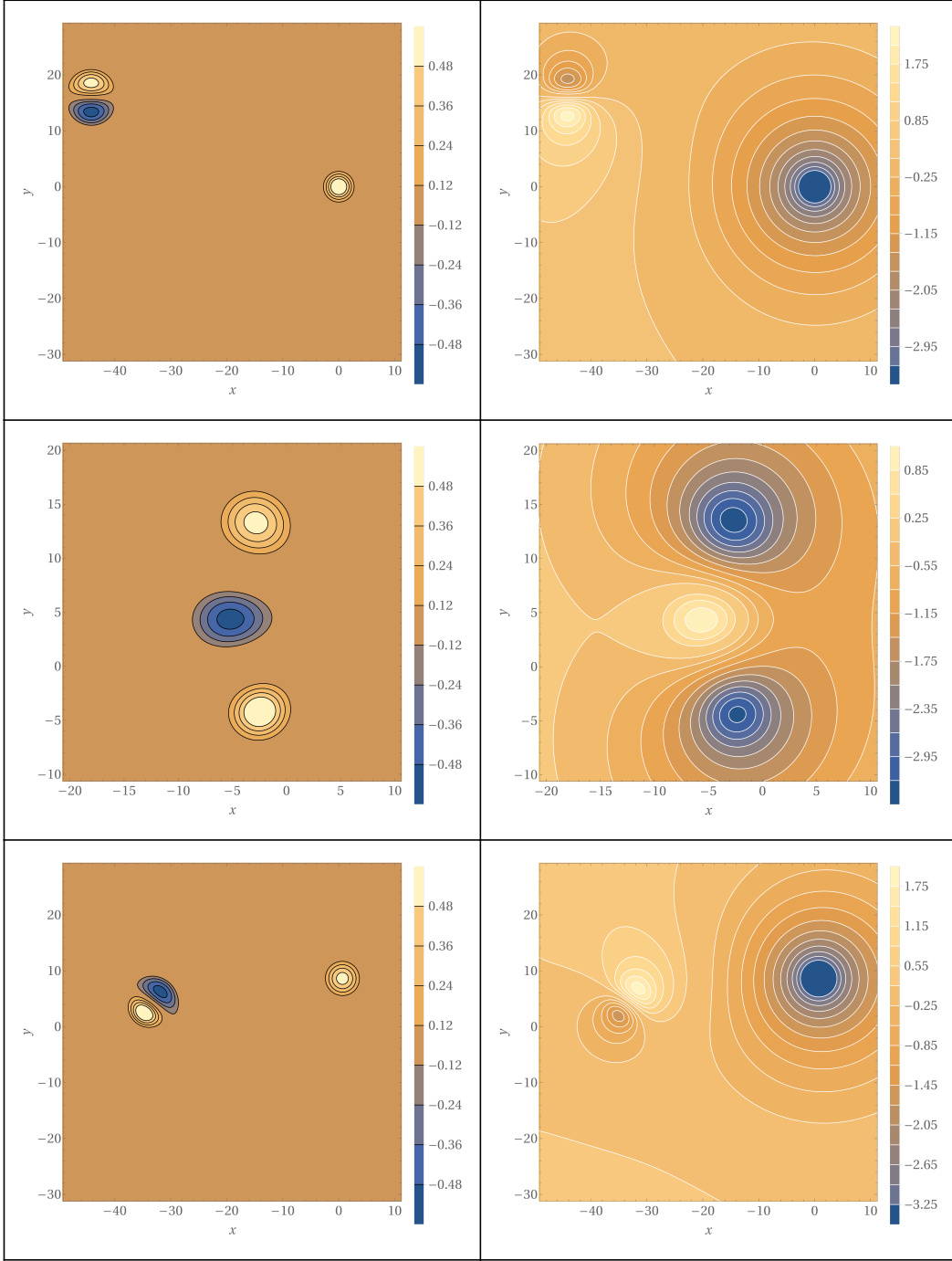
Figure B1. Time evolution of the vorticity (left) and stream function (right) of the inelastic interaction at times t=0 (top), t=70 (middle) and t=130 (bottom).

1737-1744.

Dubosq, S., & Viúdez, A. (2007). Three-dimensional mesoscale dipole frontal collisions. *Journal of Physical Oceanography*, *37*(9), 2331-2344. doi: 10.1175/JPO3105.1

Flór, J. B., & Van Heijst, G. J. F. (1994). An experimental study of dipolar vortex structures in a stratified fluid. *Journal of Fluid Mechanics*, *279*, 101133. doi: 10.1017/S0022112094003836

Huang, X., Zhang, Z., Zhang, X., Qian, H., Zhao, W., & Tian, J. (2017). Impacts of a mesoscale eddy pair on internal solitary waves in the northern South China Sea revealed by mooring array observations. *Journal of Physical Oceanography*, *47*(7), 1539-1554.

Johannessen, J., Sandven, S., Lygre, K., Svendsen, E., & Johannessen, O. (1989, 01). Three-dimensional structure of mesoscale eddies in the Norwegian Coastal Current. *Journal of Physical Oceanography - J PHYS OCEANOGR*, *19*, 3-19. doi: 10.1175/1520-0485(1989)019⟨0003:TDSOME⟩2.0.CO;2

Kloosterziel, R. C., Carnevale, G. F., & Phillippe, D. (1993, 10). Propagation of barotropic dipoles over topography in a rotating tank. *Dynamics of Atmospheres and Oceans*, *19*(1), 65-100. doi: 10.1016/0377-0265(93)90032-3

Li, Z., Wang, X., Hu, J., Andutta, F. P., & Liu, Z. (2020). A study on an anticyclonic-cyclonic eddy pair off Fraser Island, Australia. *Frontiers in Marine Science*, *7*, 1061. doi: 10.3389/fmars.2020.594358

McWilliams, J. C., & Zabusky, N. J. (1982, 01). Interactions of isolated vortices I: Modons colliding with modons. *Geophysical and Astrophysical Fluid Dynamics*, *19*(3), 207-227. doi: 10.1080/03091928208208956

Rasmussen, J., Hesthaven, J., Lynov, J., Nielsen, A., & Schmidt, M. (1996). Dipolar vortices in two-dimensional flows. *Mathematics and Computers in Simulation*, *40*(3), 207-221. doi: https://doi.org/10.1016/0378-4754(95)00033-X

Ridderinkhof, W., Le Bars, D., von der Heydt, A. S., & de Ruijter, W. P. M. (2013). Dipoles of the south east Madagascar Current. *Geophysical Research Letters*, *40*(3), 558-562. doi: https://doi.org/10.1002/grl.50157

Santiago-García, M. W., Parés-Sierra, A. F., & Trasviña, A. (2019, 12). Dipole-wind interactions under gap wind jet conditions in the Gulf of Tehuantepec, Mexico: A surface drifter and satellite database analysis. *PLOS ONE*, *14*(12), 1-23. doi: 10.1371/journal.pone.0226366

Sheres, D., & Kenyon, K. E. (1989). A double vortex along the California coast. *Journal of Geophysical Research: Oceans*, *94*(C4), 4989-4997. doi: https://doi.org/10.1029/JC094iC04p04989

Velasco Fuentes, O., & Heijst, van, G. (1995). Collision of dipolar vortices on a beta-plane. *Physics of Fluids*, *7*(11), 2735–2750. doi: 10.1063/1.868652

Viúdez, A. (2019). Exact solutions of asymmetric baroclinic quasi-geostrophic dipoles with distributed potential vorticity. *Journal of Fluid Mechanics*, *868*, R1. doi: 10.1017/jfm.2019.234

Viúdez, A. (2021). Robust and unstable axisymmetric vortices, including neutral vortices, of a new two-dimensional vortex family. *Physics of Fluids*, *33*(5), 054103. doi: 10.1063/5.0048128

Voropayev, S. I., & Afanasyev, I. D. (1992, 03). Two-dimensional vortex-dipole interactions in a stratified fluid. *Journal of Fluid Mechanics*, *236*, 665-689. doi: 10.1017/S0022112092001575

Voropayev, S. I., & Afanasyev, Y. D. (1994). *Vortex structures in a stratified fluid.* Chapman and Hall.

Wayne, C. E. (2011, 01). Vortices and two-dimensional fluid motion. *Notices of the American Mathematical Society*, *58*, 10-19.

Zavala Sansón, L., & Gonzalez, J. F. (2021). Travelling vortices over mountains and the long-term structure of the residual flow. *Journal of Fluid Mechanics*, *922*, A33. doi: 10.1017/jfm.2021.567